

Effect of Carbon Nanotube Surface Treatment on the Morphology, Electrical, and Mechanical Properties of the Microfiber-Reinforced Polyethylene/Poly(ethylene terephthalate)/Carbon Nanotube Composites

Sertan Yesil,* Goknur Bayram

Department of Chemical Engineering, Middle East Technical University, Ankara 06800, Turkey

*Present address: Department of Chemical Engineering, Kocaeli University, Kocaeli, 41380, Turkey

Correspondence to: S. Yesil (E-mail: sertan_yesil@yahoo.com)

ABSTRACT: The aim of this study is to investigate the effects of carbon nanotube (CNT) chemical properties, CNT content, and molding temperature on the morphology, electrical, and mechanical properties of the microfiber-reinforced polymer composites. These composites were prepared by extrusion and hot stretching the poly(ethylene terephthalate) (PET)/CNT phase in high density polyethylene (HDPE) matrix. Surfaces of the CNT were modified by purification with strong acid mixture (HNO_3 : H_2SO_4 mixture 1 : 1 by volume) followed by treatment with poly(ethylene glycol) (PEG). *In situ* microfibrillar composites were prepared with untreated and modified CNT. Scanning Electron Microscopy (SEM) analyses indicated that CNT were preferentially located in PET phase of the composites. SEM micrographs of the hot-stretched composites pointed out the existence of PET/CNT microfiber structure in HDPE phase up to 1 wt % CNT loadings and the electrical resistivities of these composites were lower than 10^7 ohm/cm. Tensile strength values of the composites containing 0.75 wt % CNT increased from 44 to 52 MPa after PEG treatment due to the improved mechanical strength of PET/CNT phase. © 2012 Wiley Periodicals, Inc. J. Appl. Polym. Sci. 000: 000–000, 2012

KEYWORDS: microfiber-reinforced composites; carbon nanotubes; surface treatment; mechanical strength

Received 22 November 2011; accepted 17 February 2012; published online 00 Month 2012

DOI: 10.1002/app.37518

INTRODUCTION

Polymer blends are the combination of homopolymers or copolymers, which are, in most cases, thermodynamically immiscible.¹ It has been established that fibrillar morphology can greatly improve the mechanical properties of the polymer blends when the mechanical properties of the dispersed fiber phase is higher compared with polymer matrix.² *In situ* formed microfibrils in polymer blends can be generated, by using the microfiber-reinforced composites concept, which was proposed by Evstatiev and Fakirov.³ To form a microfiber structure in a polymer blend, two polymers with different melting point temperatures should be used. Polymer with higher melting point temperature forms the dispersed microfibers in the polymer matrix with lower melting point.⁴ An elongational flow field and lower melt viscosity of the dispersed microfiber phase can accumulate the microfiber formation.⁵ In previous works, two-step strategy was used to prepare the *in situ* microfibrillar blends. During the first melt mixing and hot-stretching step at

the processing temperature of the higher melting temperature polymer, the microfibrillar morphology of this polymer is developed. Then during the second step, the blend containing microfibrils is processed through injection molding at the processing temperature of the lower melting temperature polymer and the microfibrillar structure of the dispersed phase is maintained in the structure.^{6–8}

High-performance polymer blends can be formulated by introducing particulate fillers such as titanium dioxide and carbon black into microfiber-reinforced polymer blends.^{9–14} Carbon nanotubes (CNT) can also be a good candidate as conductive filler and reinforcement material for microfibrillar polymer composites due to their unique properties such as high aspect ratio, low density, and high mechanical, thermal, and electrical properties.^{15,16} Li et al. produced CNT filled microfibrillar polymer composite based on polycarbonate and HDPE by using a shear controlled orientation in injection molding. Tensile properties of the samples were considerably increased compared to

Additional Supporting Information may be found in the online version of this article.

© 2012 Wiley Periodicals, Inc.

Table I. Physical Properties of Composite Constituents

Material	Trade name and supplier	Specifications
High density polyethylene (HDPE)	Petilen S0464; PETKİM (Turkish Petroleum Product Producer) (Turkey)	Melting temperature: 140°C
		Electrical resistivity: 10 ¹⁸ ohm/cm
		Density: 0.964 g/cm ³
Poly(ethylene terephthalate) (PET)	Melinar; AdvanSA (Turkey)	Melting temperature: 255°C
		Electrical resistivity: 10 ¹⁴ ohm/cm
		Density: 1.4 g/cm ³
Multiwalled carbon nanotubes (MWCNT)	Nanocyl 7000; Nanocyl (Belgium)	Melt flow index (2.16 kg; 190°C): 0.25–0.45 g/10 min
		Melting temperature: 255°C
		Electrical resistivity: 10 ¹⁴ ohm/cm
		Density: 1.4 g/cm ³
Multiwalled carbon nanotubes (MWCNT)	Nanocyl 7000; Nanocyl (Belgium)	Melt flow index (2.16 kg; 260°C): 20 g/10 min
		Average diameter: 10 nm
		Electrical resistivity: 10 ⁻⁴ ohm/cm
		Surface area: 250 m ² /g
Multiwalled carbon nanotubes (MWCNT)	Nanocyl 7000; Nanocyl (Belgium)	Bulk composition: 90 wt % Carbon, 10 wt % metal oxides

their conventional samples, especially in the presence of 0.5 wt % of CNT.¹⁷ Moreover, microfiber-reinforced HDPE/PET/CNT composites were prepared by using untreated CNT in one of our previous studies.¹⁸ In this study, effects of PET content and molding temperature on the morphology, electrical, and mechanical properties of the composites were investigated at a fixed CNT composition (0.5 wt %). This study showed us that, microfiber reinforcement improved the tensile and impact strength of the samples, when compared with those of blend and conventional composite systems, up to 30 wt % PET loading. However, effective improvement in mechanical properties of the composites can only be accomplished after solving the dispersion and interfacial adhesion problems of the CNT.¹⁹ In the literature, different chemical functionalization techniques have been used to improve the CNT dispersion and interfacial adhesion between the CNT and polymer matrix.^{20–22} One of these methods is the purification of CNT by using strong acid mixtures.²³ Poly(ethylene glycol) (PEG) treatment of the purified CNT (pCNT) is also a preferred method for further functionalization of the CNT surface.^{24–26} Surfaces of pCNT can interact with the hydroxyl end groups of PEG and this enhances the adhesion of PEG on the surface. However, according to the knowledge of authors there is not any study in the literature deals with the usage of surface treated CNT during the preparation of the microfiber-reinforced HDPE/PET/CNT composites; observes and explains the effects of the CNT chemical, physical structure on the properties of the microfiber-reinforced composites.

In this study, effects of CNT purification, PEG treatment, and CNT amount in the composite on the morphology, electrical, mechanical properties of the microfiber-reinforced polymer composites prepared with untreated, and modified CNT were investigated. Composites with in-situ microfiber network were prepared through extrusion and hot stretching the PET/CNT phase in HDPE matrix. Possible reasons for the differences in the morphology and properties of the composites were

explained in terms of distinctions in CNT surface properties, physical structure, and interactions between CNT and PET after the chemical treatment.

EXPERIMENTAL

Materials

In this study, poly(ethylene terephthalate) (PET) and high density polyethylene (HDPE) were used as the polymer matrices. Multiwalled CNTs (MWCNT) were used as the conductive filler. Suppliers and some physical properties of the materials are given in Table I. CNT were purified by using nitric acid (HNO₃; JT Baker 65%), sulfuric acid (H₂SO₄; JT Baker 95%) and their surfaces were treated with PEG with 1000 g/mol molecular weight (Sigma Aldrich).

Purification of CNT

In this step, 5 g portions of as-received multiwalled CNT (ASCNT) were treated with 200 mL of HNO₃ : H₂SO₄ mixture (1 : 1 by volume) in an ultrasonic bath (Bandelin Sonorex) at 80°C for 30 min. After the sonication, acid mixture was diluted with distilled water and the CNT were recovered from the solution by filtering them with the 0.2 μm pore sized filter paper. Next, hot and cold distilled water were used to wash out the residual acid on CNT. Finally, pCNT were dried in the oven for 24 h at 100°C.

Surface Treatment of CNT with PEG

During surface treatment with PEG, pCNT were dispersed in 200 mL 0.04M NiCl₂/water and 10 mL PEG were added to the solution. This mixture was sonicated in ultrasonic bath for 4 h at 80°C. At the end of the sonication, modified CNT (mCNT) were filtered, washed with distilled water, and dried at 100°C for 24 h.

Preparation and Molding of Composites

Before composite preparation, HDPE and PET pellets were dried in a vacuum oven at 60°C for 4 h and at 90°C for 24 h, respectively. During the preparation of the composites, first,

HDPE and PET were blended in a corotating twin-screw extruder (Thermoprism TSE 16 TC, $L/D = 24$) at a fixed HDPE/PET ratio (80/20 by weight), since this ratio resulted in better mechanical properties according to our previous study.¹⁸ During second extrusion HDPE/PET blends were mixed with ASCNT, pCNT, and mCNT at 0.25, 0.5, 0.75, 1, and 1.5 wt % concentrations. The HDPE/PET part was (100- x)% of the composites, where x was the CNT amount in the composites. The extrudate from the extruder die was hot stretched by using a speed adjustable engine (Siemens Micromaster 440) at a hot stretching speed of 5.8 m/min. The cross-sectional area of the extruder die was 5.7 mm² and that of the hot stretched samples were 0.3 mm², which corresponds to a hot stretching ratio (the ratio of the area of extrudate to hot stretched sample which was drawn by the engine) of 19.6.¹⁸ The stretching was performed at the room temperature, as the hot extrudate came out of the extruder die. During this procedure, no additional heating was applied. All the hot stretched samples were pelletized by using a commercial pelletizer (Thermoprism) before the molding processes. Extrusion processes were performed at a barrel temperature profile of 190–210–230–250–270°C and a screw speed of 120 rpm.

Injection and compression moldings of the composites were performed at 210°C. Furthermore, the effect of molding temperature on the composite properties was investigated by molding the microfibrillar composites at 280°C. During compression molding, samples were preheated and molded at 50 bar oil pressure for 1.5 min. and 150 bar oil pressure for 1 min, respectively. Compression molded samples were quenched to room temperature by tap water. Injection moldings (DSM Micro 10 cc Injection Molding Machine) of the samples were conducted under 15 bar pressure and at 30°C mold temperature.

Characterization of Composites

Surface energy components (γ_{solid} : total surface energy, γ_{solid}^d : dispersive component of total surface energy, γ_{solid}^p : polar component of total surface energy, γ_{solid}^A : acidic component of polar surface energy, and γ_{solid}^B : basic component of polar surface energy) of the HDPE, PET, CNT, and PET/CNT composites were determined by measuring the contact angles of probe liquids on sample surfaces. Details of surface energy measurement procedure and calculations were discussed in supporting information file which may be found in the online version of this article and in our previous studies.^{18,27} The interfacial tensions between the composite constituents (γ_{1-2}) can be determined by using the general equation with harmonic mean.

$$\gamma_{1-2} = \gamma_1 + \gamma_2 - 4\left[\frac{(\gamma_1^d \gamma_2^d)}{(\gamma_1^d + \gamma_2^d)} + \frac{(\gamma_1^p \gamma_2^p)}{(\gamma_1^p + \gamma_2^p)}\right] \quad (1)$$

Sumita et al. proposed that the selective localization of the filler in a polymer blend can be estimated by the wetting coefficient (w), which is defined by the following equation²⁷;

$$W = (\gamma_{f-B} - \gamma_{f-A})/\gamma_{A-B} \quad (2)$$

where γ_{f-A} is the interfacial tension between the polymer A and filler, γ_{f-B} is the interfacial tension between the polymer B and filler, and γ_{A-B} is the interfacial tension between two poly-

mers. If w is >1 , the filler particles locate within polymer A. If w is <-1 , the filler particles locate within polymer B. Otherwise the filler particles distribute at the interface.²⁸

Melt viscosities of the HDPE, PET, and PET/CNT composites including 1.25, 3.75, and 7.5 wt % ASCNT, pCNT, and mCNT were determined with Dynisco LCR-7001 (Capillary Viscometer) at 260°C in a shear rate range from 10 to 600 1/s. These tests were performed to demonstrate the melt viscosities of the HDPE, PET, and PET/CNT samples during the extrusion and hot stretching processes. Although HDPE/PET ratio of the HDPE/PET/CNT composite systems is constant (80/20 by weight), the CNT amount in PET phase differs as CNT composition changes from 0.25 to 1.5 wt %. Hence, the melt viscosities of PET/CNT composites containing 1.25, 3.75, and 7.5 wt % CNT were measured and illustrated. The morphological analyses of the composites were performed by using a Scanning Electron Microscope (JEOL JSM-6400). Before the morphological analyses, HDPE phase of the selected samples were etched away in hot xylene at 135°C for 45 min to observe microfibrillar morphology easier. Moreover, PET/CNT phases of some of the samples were etched away in trifluoroacetic acid at room temperature for 6 h, to determine the size of this phase. Since trifluoroacetic acid etching removes the PET/CNT phase from the composites, these phases are observed as hollow spherical particles dispersed in HDPE phase in the Scanning Electron Microscopy (SEM) micrographs. Domain sizes of the PET/CNT phases in the composites were determined from the SEM micrographs by using image analysis software (Image J).¹⁸

The electrical resistivities of the PET/CNT composites were measured with two-point probe method, which was connected to a Keithley 2400 constant current source meter. The volume resistivity, ρ was calculated from the relationship:

$$\rho = (V/I) \times (S/L) \quad (3)$$

in which V was the voltage drop, I was the current, L was the length, and S was the cross sectional area of the sample.

The mechanical properties were investigated by using a Shimadzu Autograph AG-100 KNIS MS universal tensile testing instrument, according to ISO 527-2 5A standards. Tensile specimens had a thickness of 2 mm, a width of 4 mm, and a gauge length of 20 mm. According to the gauge length and a strain rate of 0.1 min⁻¹, the crosshead speed of testing instrument was selected as 2 mm/min. Impact strength of the samples were determined by using a Ceast Resil Impactor 6967 impact testing device equipped with a charpy apparatus according to ASTM D 5942 standards, instrumented with a 7.5 J hammer. The impact specimens had a thickness of 4 mm, a width of 10 mm and a length of 80 mm. Five specimens of each sample were tested and the average of these tests were reported with standard deviations in both tensile and impact characterizations.

RESULTS AND DISCUSSION

Location of CNT in the Composites

Surface energies of the polymers and conductive filler; mainly determine the location of the conductive filler in the composite.

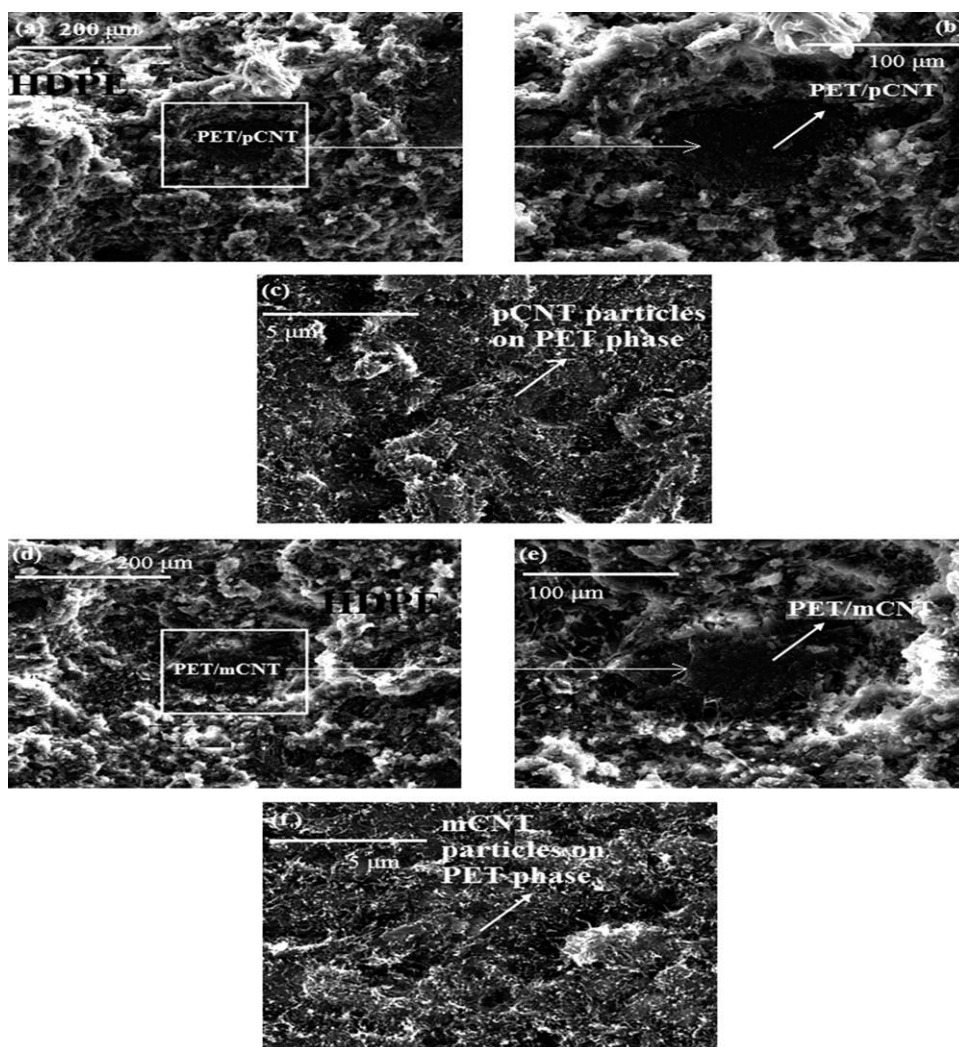


Figure 1. SEM micrographs of the HDPE/PET/CNT composite systems (molded at 280°C and show the selective localization of pCNT and mCNT in PET phase); (a, b, and c) composite containing 0.5 wt % pCNT [(b) is the magnified micrograph of the rectangular region in (a); (c) is the magnified PET/pCNT phase in (b)], (d, e, and f) composite containing 0.5 wt % mCNT [(e) is the magnified micrograph of the rectangular region in (d); (f) is the magnified PET/mCNT phase in (e)].

Surface energy components of the composite constituents are calculated in our previous studies.^{18,29} After the determination of the surface energy components for each material, surface tensions between the composite constituents are calculated by using eq. 1. Wetting coefficient (w) calculations were performed by using the surface tensions between the composite constituents, to determine the location of CNT in the composites theoretically. The wetting coefficients for HDPE/PET/ASCNT, HDPE/PET/pCNT, and HDPE/PET/mCNT composites are calculated as 1.27, 1.46, and 1.37, respectively, from eq. 2. It is observed that CNT particles should disperse in PET phase theoretically since the wetting coefficients for the composites prepared with all types of CNT are >1 . Wetting coefficients for pCNT and mCNT are greater than that of ASCNT due to the enhanced interactions between CNT and PET after the surface treatment. Because of the possible chemical affinity between PEG and HDPE due to the common ethylene parts in their chemical structures, the wetting coefficient

of mCNT is lower than that of pCNT. Moreover, the incorporation of the nanoparticles into polymer blends can increase the compatibility of polymer phases by decreasing the interfacial tension between the phases.⁹ Interfacial tensions between the HDPE and PET/CNT phases in HDPE/PET/ASCNT, HDPE/PET/pCNT, and HDPE/PET/mCNT composites are calculated as 5.82, 5.04, and 4.03 mN/m, respectively. The interfacial tensions between the PET/CNT phases and HDPE are lower in the composites prepared with surface treated CNT when compared with ASCNT based composite, which might show the enhanced miscibility between these phases.

The preferential distribution of the pCNT and mCNT in PET phase of HDPE/PET/CNT composites can also be observed in Figure 1. In these micrographs, CNT particles are located on the surfaces of the PET phases as fibrillar nanoparticles. These results are also coherent with the theoretical wetting coefficient

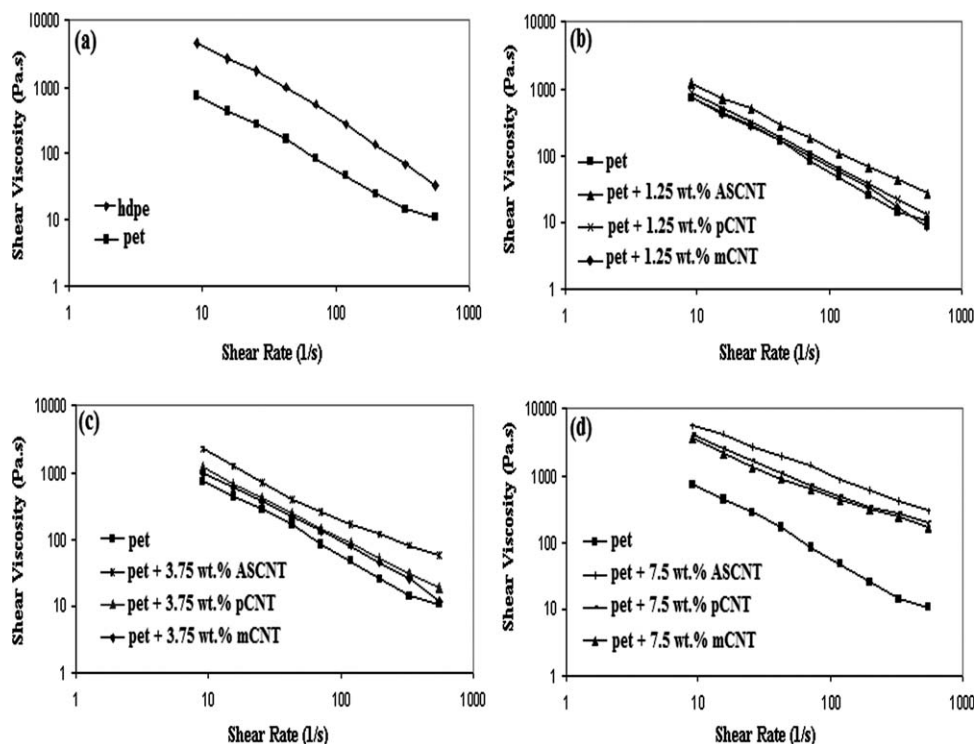


Figure 2. Shear viscosity versus shear rate graphs for HDPE, PET, and PET/CNT composites; (a) HDPE and PET and (b) PET and PET/CNT composites containing 1.25 wt % CNT, (c) PET and PET/CNT composites containing 3.75 wt % CNT, and (d) PET and PET/CNT composites containing 7.5 wt % CNT.

calculations and previous findings, which suggest that carbon based conductive filler particles, prefer to locate in the phases with lower melt viscosity of polymer blends.³⁰ Capillary viscometer analyses show that PET has much lower melt viscosity than HDPE at the composite mixing temperature (Figure 2), which is also a requirement for the formation of the satisfactory microfibers in an immiscible blend. The selective dispersion of

ASCNT in PET phase of HDPE/PET/CNT composites was shown in one of our previous study.¹⁸

Morphology Studies

The distribution and average domain sizes (d_{avg}) of the PET/CNT phases in HDPE matrix for HDPE/PET/CNT composites can be observed in Figure 3. Micrographs exhibit that the PET/

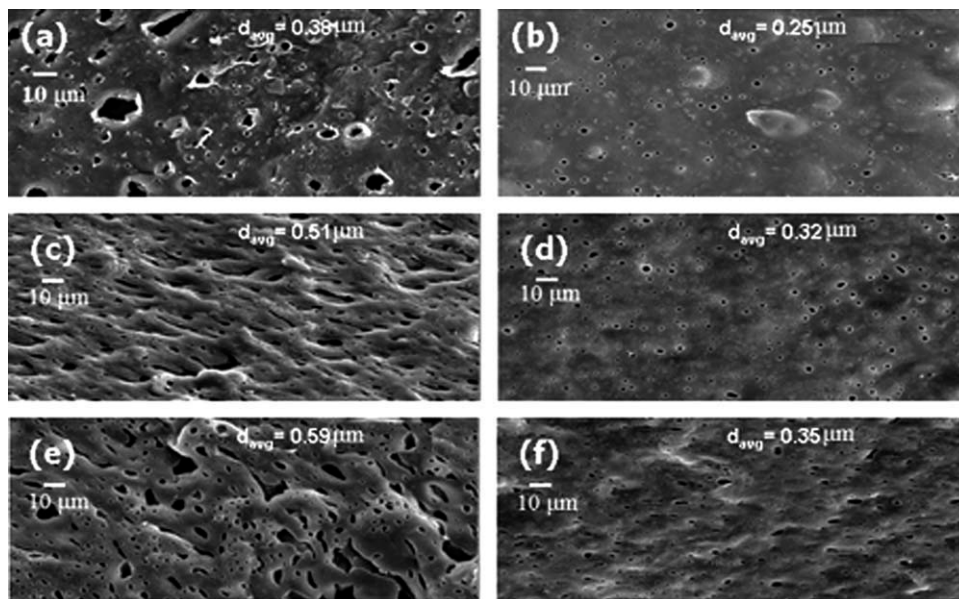


Figure 3. SEM micrographs of the HDPE/PET/CNT composites (a) 0.25 wt % ASCNT, (b) 1.5 wt % ASCNT, (c) 0.25 wt % pCNT, (d) 1.5 wt % pCNT, (e) 0.25 wt % mCNT, and (f) 1.5 wt % mCNT (samples were directly taken from the extruder die without hot-stretching and etched with trifluoroacetic acid).

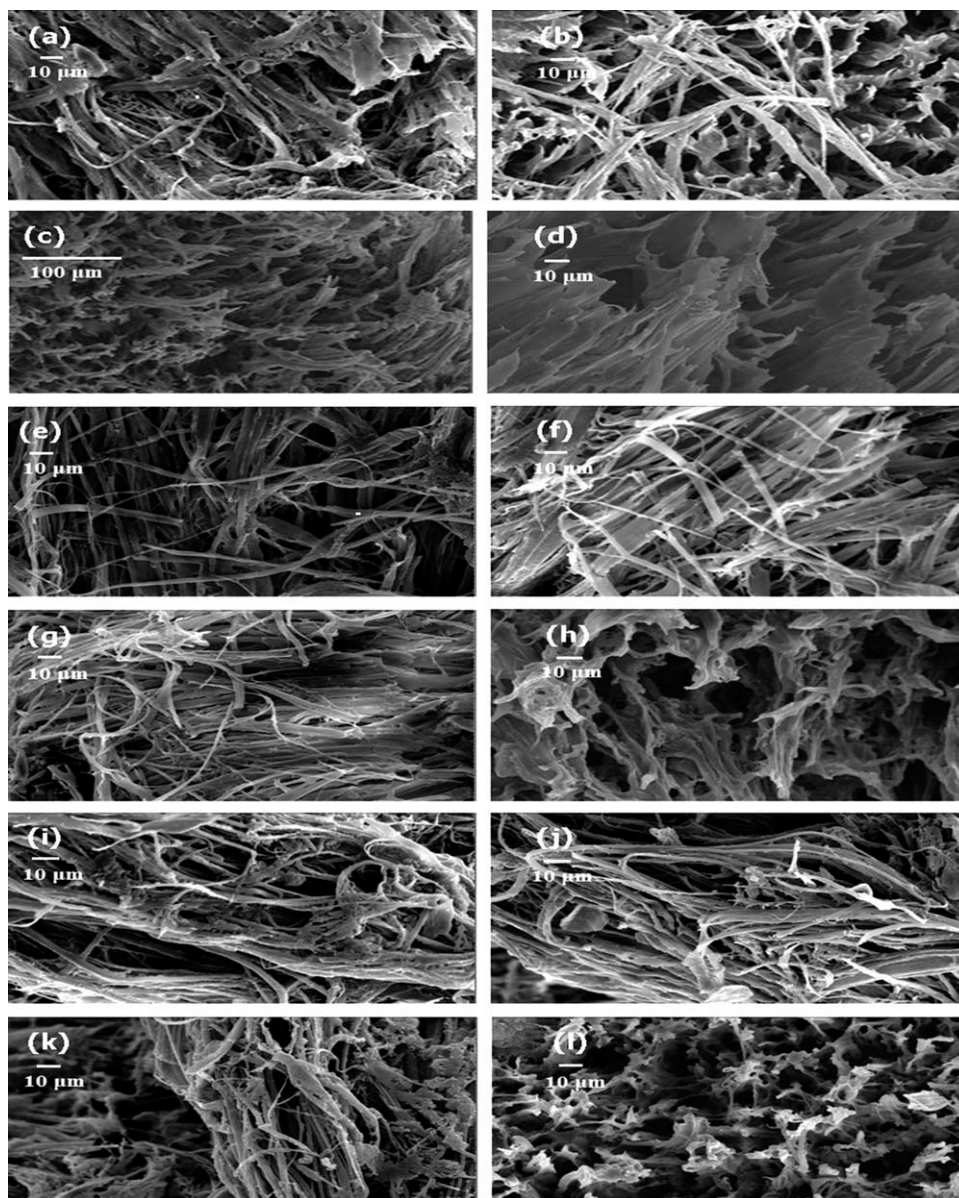


Figure 4. SEM micrographs of the hot-stretched HDPE/PET/CNT composites (a) 0.25 wt % ASCNT, (b) 0.5 wt % ASCNT, (c) 1 wt % ASCNT, (d) 1.5 wt % ASCNT, (e) 0.25 wt % pCNT, (f) 0.5 wt % pCNT, (g) 1 wt % pCNT, (h) 1.5 wt % pCNT, (i) 0.25 wt % mCNT, (j) 0.5 wt % mCNT, (k) 1 wt % mCNT, and (l) 1.5 wt % mCNT (etched with hot xylene).

CNT phase is dispersed in the HDPE phase. As a result of the reduction in the coalescence of the PET phase in the presence of the higher amount of rigid CNT particles,³¹ the average sizes of PET/CNT phases in 1.5 wt % CNT containing composites are lower than those of 0.25 wt % CNT containing composites for all types of CNT. PET/CNT phases seem to be dispersed more homogeneously for pCNT and mCNT based composites when compared with ASCNT based composites (Figure 3). However, the average PET/CNT phase sizes of the pCNT and mCNT based composites are larger than that of ASCNT based composite at the same CNT loadings. The reason for this might be the lower melt viscosity of the PET/CNT phase filled with the surface treated CNT (Figure 2),³² which

causes a decrease in the PET/CNT phase coalescence, during processing of composites.³¹

Deformation of PET/CNT phase into microfibers during elongational flow strongly depends on the melt viscosity of the dispersed phase. Moreover, the fibrillation of the PET phase in the presence of CNT particles also depends on the concentration of CNT in this phase. Micrographs of the hot-stretched HDPE/PET/CNT composites [Figure 4(a–d)] show the *in situ* PET/ASCNT microfiber structure in HDPE phase up to 0.75 wt % CNT composition (3.75 wt % CNT loading in PET phase). After this amount of CNT loading, increase in the melt viscosity of PET/ASCNT phase limits the microfiber formation due to the restrictions during deformation of the PET/CNT phase into

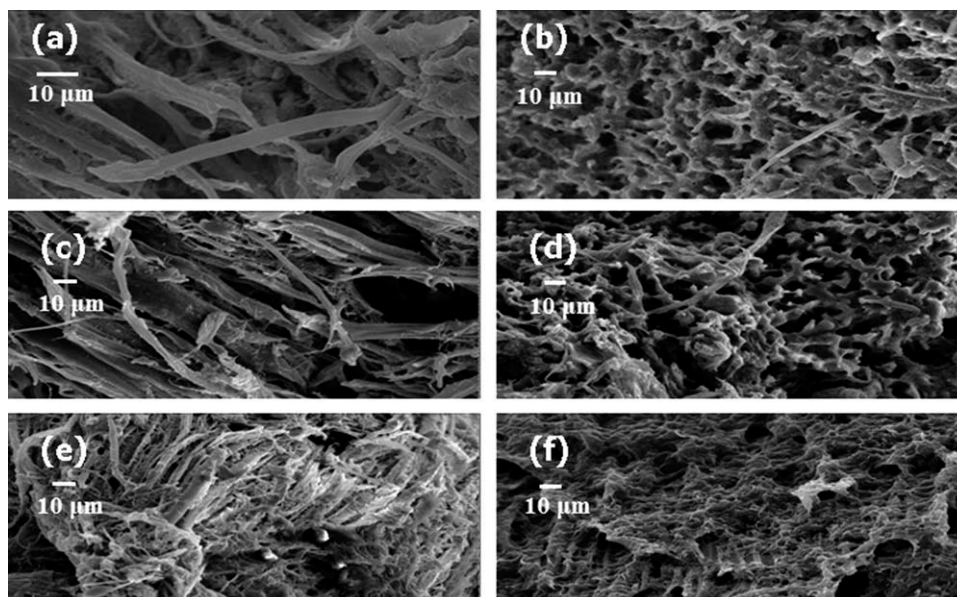


Figure 5. SEM micrographs of the microfibrillar HDPE/PET/CNT composites (a) 0.25 wt % ASCNT, (b) 1.5 wt % ASCNT, (c) 0.25 wt % pCNT, (d) 1.5 wt % pCNT, (e) 0.25 wt % mCNT, and (f) 1.5 wt % mCNT (molded at 210°C and etched with hot-xylene).

microfibers in the presence of rigid CNT particles. However, hot-stretched HDPE/PET/CNT composites prepared with surface treated CNT show the successful formation of PET/CNT microfibrillar structure in HDPE phase up to 1 wt % CNT loading [Figure 4(e-l)]. Melt viscosities of the composites including pCNT and mCNT are lower than those of ASCNT containing composites at all compositions (Figure 2). The formation of microfibers are more effective at higher concentrations of pCNT and mCNT when compared to ASCNT due to the remarkable melt viscosity difference between the PET/pCNT, PET/mCNT composites, and PET/ASCNT composite for all CNT loadings. The smaller PET/CNT phase sizes of the 1.5 wt % CNT containing composites for all types of CNT with respect to the lower amount of CNT loadings (0.25 wt %; Figure 3), restrict the longer microfiber formation since narrower PET/CNT droplets deform into shorter microfibers during hot-stretching and a successful microfibrillar network can not be obtained inside the composite [Figure 4(d,h,l)]. The SEM micrographs of the injection molded (210°C) specimens of the microfiber-reinforced composites [Figure 5(a,c,e)] reveal that the well defined microfibrillar structure is preserved for the composites in which the microfiber formation was successful. However, micrographs of the molded (210°C) composites with inefficient microfiber formation (1.5 wt % CNT composition) display only a few microfibers in their micrographs [Fig 5(b,d,f)].

Electrical Resistivity Measurements

In the microfibrillar HDPE/PET/CNT system, the percolation threshold depends on the percolation threshold of CNT particles in PET phase and the percolation threshold of PET/CNT phase in the HDPE matrix.³⁰ It is known that PET/CNT composites have very high electrical conductivity and low percolation threshold concentration. The electrical resistivity values of the PET/CNT composites prepared with ASCNT, pCNT, and mCNT are $<10^6$ ohm/cm at 0.25 wt % CNT loading, which

shows that the percolation threshold concentration of these composite systems are lower than this CNT concentration. Thus, electrical resistivity values of the composites pass from insulator range to semiconductor range ($<10^8$ ohm/cm) [Figure 6(a)], when PET/CNT phase forms a continuous microfibrillar structure in HDPE matrix. The current conduction is easier since the microfibers with high electrical conductivity can contact with each other directly when the continuous microfiber network is formed in the composite. Moreover, electrical resistivities of the composites decrease with the increasing amount of conductive filler until the microfiber network is present in the composites. However, microfiber-reinforced composites, which do not have a successful microfiber structure have higher electrical resistivities than those of the ones with microfibrillar morphology. The electrical resistivity value of the HDPE/PET/ASCNT composite is between 10^5 and 10^6 ohm/cm at 0.75 wt % ASCNT composition. However, it increases to 10^9 ohm/cm when ASCNT content in the composite is 1 wt % due to the lack of well defined conductive microfiber network inside the composite (Figures 4 and 5). The same characteristic is also observed for pCNT and mCNT based composites. There is a remarkable change in the electrical resistivity values of these composites between 1 and 1.5 wt % CNT loadings. The existence of the well-defined microfibers at higher CNT contents for the surface treated CNT results in lower electrical resistivity values at higher CNT compositions when compared with those of the ASCNT filled composites (Figures 4 and 5).

ASCNT based composites generally have lower electrical resistivity values than those of the composites based on the other two CNT up to 1 wt % CNT loading. The higher intrinsic electrical resistivities of the purified and modified CNT when compared with ASCNT causes a decrease in the electrical conductivities of PET/CNT phases prepared with surface treated CNT. Because of the surface treatment, oxygen containing functional groups and

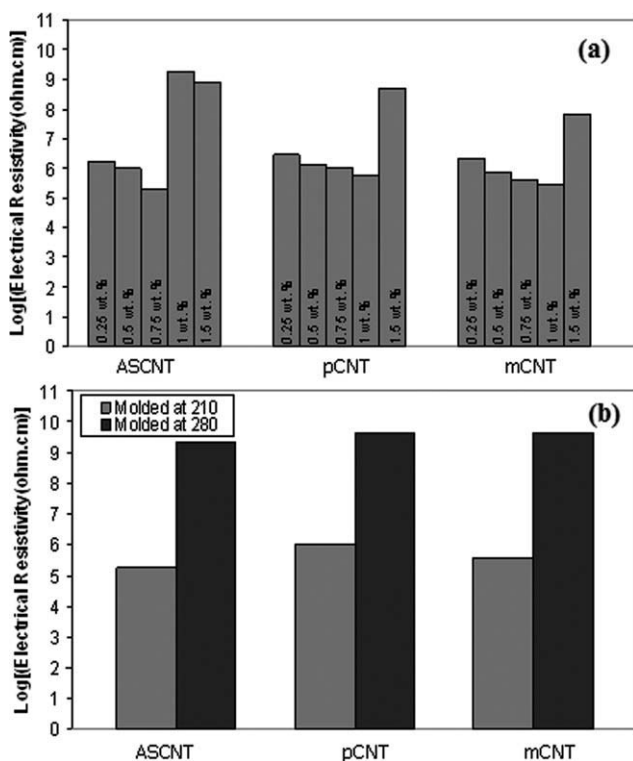


Figure 6. Electrical resistivity values of the microfibrillar HDPE/PET/CNT composites; (a) effect of CNT surface treatment and amount (molded at 210°C), and (b) effect of molding temperature at 0.75 wt % CNT containing microfibrillar composites.

defects on the surface of CNT (check the results of the Fourier Transformed Infrared Spectroscopy (FTIR), X-Ray Diffraction (XRD), Scanning Electron Microscopy (SEM) and Thermal Gravimetric (TGA) analyses of the CNT samples, given in the supporting information file) might damage the perfect electronic structure of the CNT. Insulating oxide and PEG region on the surface does not allow the transportation of electrons effectively and this decreases the electrical conductivity of the individual CNT aggregates.^{33,34} The electrical resistivity value of the 0.75 wt % ASCNT containing microfibrillar composite is approximately two times lower than that of the mCNT based composite [Figure 6(b)]. Molding temperatures above the melting point of PET (255°C) cause PET/CNT phase to melt and loose the microfiber characteristics since, as the microfiber phases melt, they have a spherical shape thermodynamically. Because of this, PET/CNT phases are dispersed in the HDPE phase and a co-continuous morphology cannot be obtained (Figures 1 and 3). Composites molded at higher temperature do not have a continuous PET/CNT network in their structures at 80/20 (HDPE/PET) ratio and microfiber-reinforced composites molded at 210°C have lower electrical resistivity values than those of the composites molded at 280°C for all CNT types [Figure 6(b)].

Mechanical Properties

The intrinsic mechanical properties of the matrix and microfiber phase; shape of the PET/CNT phase; degree of interfacial adhesion between the HDPE matrix and microfibrillar PET/CNT phase mainly determine the mechanical properties of the microfiber-reinforced HDPE/PET/CNT composites. Reinforcing

effect of the microfibers with advanced mechanical strength can enhance the mechanical properties of the microfibrillar composites more effectively. Microfiber formation in the presence of CNT particles improves the tensile strength and modulus when compared with those of the microfibrillar HDPE/PET blend (Figure 7). However, this reinforcement is limited for the ASCNT based composites due to the lower tensile properties of PET/ASCNT phase than PET/pCNT and PET/mCNT phases. PET/ASCNT composites generally suffer from the weak mechanical properties due to the weak interfacial adhesion between PET and CNT, which causes debonding and pull outs of CNT from the surrounding matrix.³⁵ After purification, carboxyl and hydroxyl groups formed on the CNT surface (check the results of the FTIR and TGA analyses of the CNT samples, given in the supporting information file) can react with the carboxyl end groups of PET and increase the chemical compatibility in the

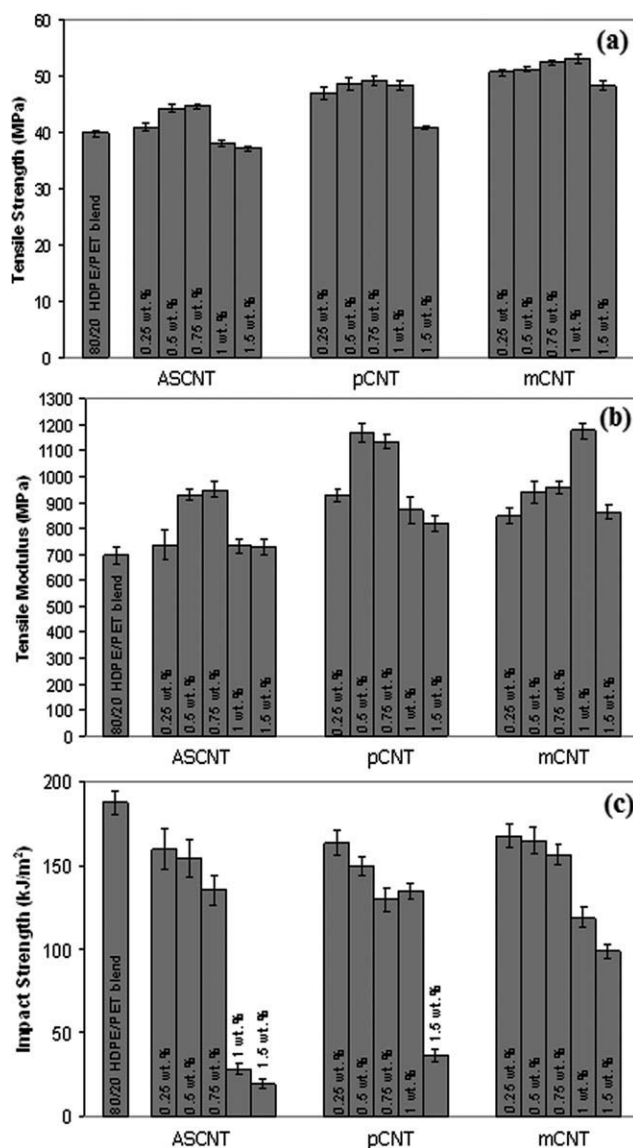


Figure 7. Mechanical properties of the microfibrillar HDPE/PET/CNT composites and HDPE/PET blend; (a) tensile strength values, (b) tensile modulus values, and (c) impact strength values.

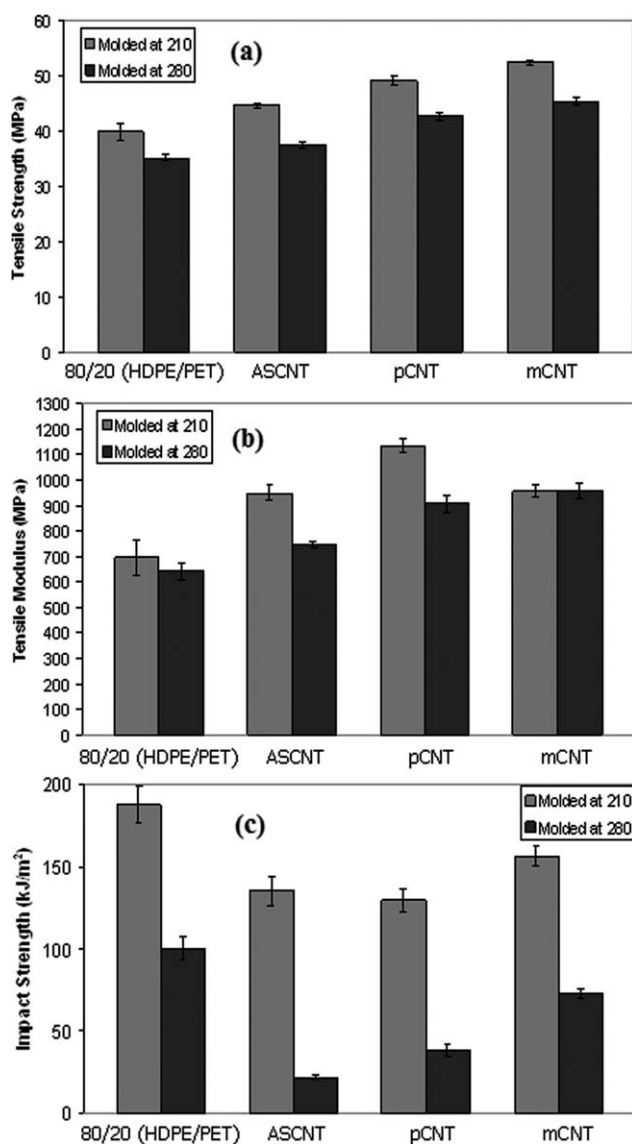


Figure 8. Mechanical properties of the microfibrillar HDPE/PET/CNT composites containing 0.75 wt % CNT and HDPE/PET blends (effect of molding temperature); (a) tensile strength values, (b) tensile modulus values, and (c) impact strength values.

composite. Moreover, defect sites on the CNT surface can increase the mechanical interlocking and covalent bonding between CNT and PET matrix. PEG treated CNT also has different modes of reaction patterns with PET. The hydroxyl end groups of PEG can interact with the carboxyl end groups and aromatic group of PET. These interactions between composite constituents improve the efficiency of load transfer from the PET to CNT³⁶ and mechanical strength of the composites prepared with pCNT and mCNT might be higher than those of PET/ASCNT composite. As a result of these effects, tensile strength values of the pCNT and mCNT based composites are higher than those of the ASCNT containing composites for all CNT compositions.

Similar with the electrical resistivity results, generally a sharp decrease is observed for tensile modulus and impact strength

values of the microfiber-reinforced composites after 0.75 or 1 wt % CNT loading due to the limited microfiber formation in these composites (Figures 4 and 5) and this decrease in the amount of microfibrils in the structure diminishes the reinforcing effect of this phase. Tensile modulus values of the 0.75 and 1 wt % pCNT containing composites are 1130 and 870 MPa, respectively. Microfibrils present in the composite, decrease the crack formation and propagation in the sample during the impact test.³⁷ So, when the microfiber concentration in the composite decreases, a sudden decrease in the impact strength is also observed for all types of CNT. Impact strength values of the 0.75 and 1 wt % ASCNT containing composites are 135 and 30 kJ/m², respectively (Figure 7). Molding temperature increment decrease the mechanical properties of the microfiber-reinforced composites due to the melting of PET/CNT phase (Figure 8). During the molding of the composites at 280°C, PET/CNT microfibrils with high aspect ratio transform into spherical particles with lower aspect ratio (Figure 1), and the reinforcing effect of this phase descends.

CONCLUSIONS

Preferential localization of all types of CNT in PET phase of the HDPE/PET/CNT composites, which was shown by the wetting coefficient calculations and SEM micrographs of the composites resulted in enhanced electrical conductivity values due to the co-continuous morphology induced by the well defined microfibrillar network. Sharp decreases in electrical conductivity, tensile modulus, and impact strength values of the composites were observed after 0.75 and/or 1 wt % CNT contents for ASCNT and pCNT, mCNT, respectively, owing to the limited microfiber formation which was revealed by the SEM micrographs of the hot stretched composite samples. The increase in the melt viscosity of the PET/CNT phase at higher CNT compositions inhibited the efficient formation of PET/CNT microfibrils in the composites. Electrical resistivity and tensile strength values of the composites prepared with pCNT and mCNT were higher than those of ASCNT based composites due to the lower melt viscosity and better intrinsic properties of the PET/CNT phase containing surface treated CNT.

REFERENCES

- Guerrero, C.; Lozano, T.; Gonzalez, V.; Arroyo, E. *J. Appl. Polym. Sci.* **2001**, *82*, 1382.
- Xu, H. S.; Li, Z. M.; Yang, S. Y.; Pan, J. L.; Yang, W.; Yang, M. B. *Polym. Eng. Sci.* **2005**, *45*, 1231.
- Evstatiev, M.; Fakirov, S. *Polymer* **1992**, *33*, 877.
- Li, Z. M.; Yang, M. B.; Xie, B. H.; Feng, J. M.; Huang, R. *Polym. Eng. Sci.* **2003**, *43*, 615.
- Zhong, G. J.; Li, Z. M.; Li, L. B.; Mendes, E. *Polymer* **2007**, *48*, 1729.
- Fakirov, S.; Evstatiev, M.; Friedrich, K. *Polymer Blends To Microfibrillar Reinforced Composites*; Wiley: New York, **2000**.
- Lin, X. D.; Cheung, W. L. *J. Appl. Polym. Sci.* **2003**, *88*, 3100.

8. Zhong, G. J.; Li, Z. M.; Li, L.; Shen, K. *Polymer* **2008**, *49*, 4271.
9. Li, W.; Schlarb, A. K.; Evstatiev, M. *J. Appl. Polym. Sci.* **2009**, *113*, 1471.
10. Xu, X. B.; Li, Z. M.; Yu, R. Z.; Lu, A.; Yang, M. B.; Huang, R. *Macromol. Mater. Eng.* **2004**, *289*, 568.
11. Mallette, J. G.; Quej, L. M.; Marquez, A.; Manero, O. *J. Appl. Polym. Sci.* **2001**, *81*, 562.
12. Dai, K.; Xu, X. B.; Li, Z. M. *Polymer* **2007**, *48*, 849.
13. Garmabi, H.; Naficy, S. *J. Appl. Polym. Sci.* **2007**, *106*, 3461.
14. Naficy, S.; Garmabi, H. *Comp. Sci. Tech.* **2007**, *67*, 3233.
15. Ajayan, P. M.; Schadler, L. S.; Giannaris, C.; Rubio, A. *Adv. Mater.* **2000**, *12*, 750.
16. Thostenson, E. T.; Chou, T. W. *J. Phys. D: Appl. Phys.* **2003**, *36*, 573.
17. Li, S. N.; Li, B.; Li, Z. M.; Fu, Q.; Shen, K. *Z. Polymer* **2006**, *47*, 4497.
18. Yesil, S.; Koysuren, O.; Bayram, G. *Polym. Eng. Sci.* **2010**, *50*, 2093.
19. Kathi, J.; Rhee, K. Y.; Lee, J. H. *Compos. A* **2009**, *40*, 800.
20. Gojny, F. H.; Schulte, K. *Comp. Sci. Tech.* **2004**, *64*, 2303.
21. Wang, Y. B.; Iqbal, Z.; Malhotra, S. V. *Chem. Phys. Lett.* **2005**, *402*, 96.
22. Zheng, Y. P.; Zhang, A. B.; Chen, Q. H.; Zhang, J. X.; Ning, R. C. *Mater. Sci. Eng. Part A* **2006**, *435–436*, 145.
23. Spitalsky, Z.; Krontiras, C. A.; Georga, S. N.; Galiotis, C. *Compos. A* **2009**, *40*, 778.
24. Blighe, F. M.; Blau, W. J.; Coleman, J. N. *Nanotechnology* **2008**, *19*, 415709.
25. Wang, Y.; Xiong, H.; Gao, Y.; Li, H. *J. Mater. Sci.* **2008**, *43*, 5609.
26. Cordella, F.; De Nardi, M.; Menna, E.; He'bert, C.; Loi, M. A. *Carbon* **2009**, *47*, 1264.
27. Koysuren, O.; Yesil, S.; Bayram, G. *J. Appl. Polym. Sci.* **2007**, *104*, 3427.
28. Feng, J.; Chan, C. M.; Li, J. X. *Polym. Eng. Sci.* **2003**, *43*, 1058.
29. Yesil, S.; Bayram, G. *Polym. Eng. Sci.* **2011**, *51*, 1286.
30. Xu, X. B.; Li, Z. M.; Yang, M. B.; Jiang, S.; Huang, R. *Carbon* **2005**, *43*, 1479.
31. Foulger, S. H. *J. Polym. Sci. Part B: Polym. Phys.* **1999**, *37*, 1899.
32. Jiang, G.; Huang, H. X. *J. Appl. Polym. Sci.* **2009**, *114*, 1687.
33. Liu, F.; Zhang, X.; Li, W.; Cheng, J.; Tao, X.; Li, Y.; Sheng, L. *Compos. A* **2009**, *40*, 1717.
34. Barros, E. B.; Souza, A. G.; Lemos, V.; Filho, J. M.; Fagan, S. B.; Herbst, M. H.; Rosolen, J. M.; Luengo, J. A.; Huber, J. G. *Carbon* **2005**, *43*, 2495.
35. Jin, S. H.; Yoon, K. H.; Park, Y. B.; Bang, D. S. *J. Appl. Polym. Sci.* **2008**, *107*, 1163.
36. Wang, M.; Pramoda, K. P.; Goh, S. H. *Carbon* **2006**, *44*, 613.
37. Meincke, O.; Kaempfer, D.; Weickmann, H. *Polymer* **2004**, *45*, 739.